Recharging Processes of Ce^{3+} in Gamma-irradiated YAG:Ce Single Crystals[1]

T. Butaeva[a][*]**, I. Ghambaryan**[a]**, and M. Mkrtchyan**[b]

[a]*Institute for Physical Research, National Academy of Sciences, Ashtarak-2, 0203 Armenia*
[b]*National Science Laboratory, Yerevan, 0036 Armenia*
[*]*e-mail: tbutaeva@gmail.com*
Received August 11, 2014

Abstract—The influence of γ-irradiation on the spectral properties of YAG and YAG:Ce (~0.12 and ~0.2 at %) single crystals is studied. The interrelation between the changes of γ-induced absorption of Ce^{3+} and of some color centers in the crystals is established. It is shown that the analysis of radiative behavior of Ce^{3+} in YAG:Ce crystals gives the opportunity: to evaluate a quantity of electron−hole traps influencing on cerium ions in as-grown crystals and involving in radiation processes of cerium ions recharging; to predict the concentration changes of Ce^{3+} in the crystals irradiated by doses $(1.13–5.5) \times 10^7$ rad of γ-rays. The reasons of the activator ions concentration impact on the various radiation behaviors of γ-induced absorption and optical quality of these crystals are discussed.

INTRODUCTION

Single crystalline bulk $Y_3A_5O_{12}$:Ce (YAG:Ce) [1, 2] is a well-established and industrially produced scintillator possessing high light yield (20000−24000 ph/MeV), moderate decay time (10−120 ns), good energy resolution (~7%) and used for applications in X-ray and low (<300 keV) energy γ-ray detectors [3]. However, high-quality crystals production is conjugated with a range of issues one of which is a definition of quantity and types of charge traps existing in as-grown crystals. Presence of hole (h) and electron (e) traps and of other structural defects in this oxide material is a reason of the occurrence of unwanted absorptions induced by radiation in the range of emission and a formation of additional relaxation channels [4]. Moreover, ability of Ce^{3+} ions to be easily recharged and ionic radiuses misfit of Ce^{3+} and Y^{3+} leads to appearance in these crystals of unstable valence states of the regular activator ions. Formation of (Ce^{3+} + h) and (Ce^{4+} + e) centers which can strongly change the efficiency of color centers generation under an influence of radiation (γ-, X-rays) in different glasses had been considered in detail in [5, 6]. Occurrence of the same centers in YAG:Ce crystals had been discussed in [7]. Existence of such bound states of cerium ions in the crystals is the reason of origin of γ-induced Ce^{4+} ↔ Ce^{3+} recharging processes which leads to variations in the Ce^{3+} concentration: increase in final concentration of the activator in YAG:Ce with small initial Ce^{3+} con-

tent and ionization of Ce^{3+} for the crystals with higher Ce^{3+} content [8]. Accordingly, the imperfection level of the crystal after irradiation strongly depends not only on its initial quality and also on the concentration of active dopant [9]. Another type of defects caused by the activator ions is substitution defect, so-called "antisite" Ce$^{3+}_{Al}$ center observed in garnet [8, 10, 11] and perofskite [12] crystals. It has been noted [11] that existence of Ce$^{3+}_{Al}$ in LuAG:Ce (8 and 550 at ppm) can reduce the scintillation efficiency of the crystals and negatively influence on their scintillation characteristics.

Thus, the evaluation of color centers quantity affecting the activator ions in YAG:Ce crystals and influence of Ce^{3+} concentration on the crystals quality still are important today. Purpose of this work includes: definition of some color centers participating in changes of Ce^{3+} absorption in γ-irradiated YAG:Ce crystals; search of an assessment manner of the quantity of charge traps interacting with the activator ions in as-grown and irradiated crystals; determination of the reasons of opposite behavior of γ-induced absorption of Ce^{3+} in the crystals with different concentration (~0.12 and ~0.2 at %) of the activator ions.

USED MATERIALS AND RESEARCH METHODS

YAG and YAG:Ce single crystals (SC) were grown by the vertical Bridgman method (Laboratory of Luminous Materials, IPR NAS RA). Two groups of

---

[1] The article is published in the original.

Table 1. Applied and absorbed doses of γ-rays, number of γ-photons absorbed by cerium ions in YAG:Ce crystals (SC1 and SC2)

Dose, D	D_{dos}, 10^7 rad	D_{abs}, 10^7 rad	SC1 N_{abs}(Ce), 10^{11} γ-photons	SC2 N_{abs}(Ce), 10^{11} γ-photons
1	1.13	0.96	1.45	1.40
2	3.10	2.56	3.92	3.70
3	5.50	4.69	7.41	6.90

crystal plates (0.1 mm thickness) of YAG:Ce (0.12; 0.13; 0.13 at %) and YAG:Ce (0.18; 0.2; 0.22 at %), hereinafter marked as SC1 and SC2 respectively, have been chosen for experimental studies. Volumes relation of the crystal plates of SC1 to SC2 ones was 1.04–1.08. Activator concentration (C_{Ce}) in the crystals was estimated by the absorption coefficient magnitudes of Ce^{3+} [13]. Optical density (D) spectra of the crystals were recorded at room temperature in the range of 189–900 nm by the spectrophotometer "SPECORD M40" and the absorption coefficient k has been deduced considering the sample thickness. Investigated crystals were irradiated by three different doses (D_{dos}) from γ-source of ^{60}Co (photon energy −1.25 MeV) at dose rate of 28 rad/s. The true radiation doses absorbed by the crystals have been calculated [14] by

$$D_{abs} = [(\mu/\rho)_{abs}/(\mu/\rho)_{dos}] D_{dos},$$

where D_{abs} is the energy dose absorbed by a sample, D_{dos} is the energy dose absorbed by a dosimetric system, $(\mu/\rho)_{dos}$ is the mass absorption coefficient of the dosimeter (0.02950 cm²/g) for the used source,
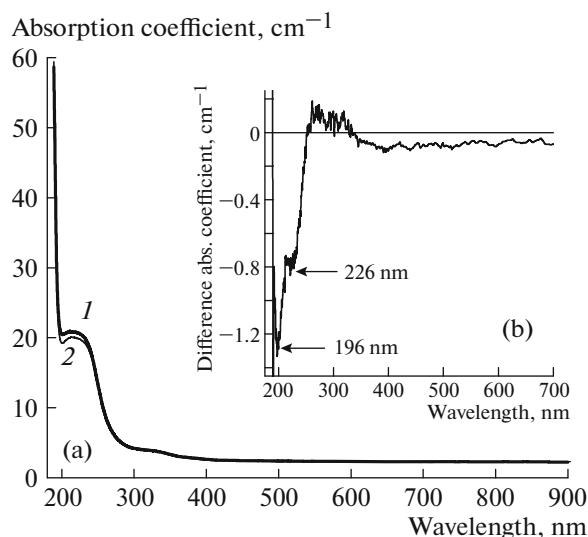
$(\mu/\rho)_{abs}$ is the mass energy-absorption coefficient [15] of the sample. For SC1 and SC2, the applied doses of γ-radiation, calculated absorbed doses and number of γ-photons absorbed by cerium N_{abs}(Ce) in these crystals are presented in Table 1.

RESULTS AND DISCUSSION

Color Centers Absorption in YAG and YAG:Ce

Observed in our measurements the absorption of color centers, formed in YAG and YAG:Ce crystals, are considered in this division.

The absorption spectrum of as-grown YAG crystal (Fig. 1a) shows a presence of significant absorption at <200 nm, intense band at ~210 nm and more weakly band at ~320 nm. A shape and an intensity of the absorption at 190–240 nm as well as some distinctions in the range 240–330 nm depend on the crystals growing technique and a purity of row materials [16–18].

Gamma irradiation of YAG by dose 2 (Fig. 1a) improves the crystal transmission except the range at 250–320 nm (Fig. 1b). This range corresponds to the absorption of uncontrollable impurity ions of the transition metals such as $Fe^{2, 3+}$, Cr^{3+} [8, 9, 16, 19] replacing Al^{3+} ions in octahedral sites of the crystal. Instead of the broad absorption band at ~210 nm, in γ-induced spectra appears a decreased absorption of two bands at 196 and 226 nm associated with F and F^+ centers in [20]. The maximal change of γ-induced absorption at <190 nm is observed in the range of the crystal's excitons creation [21].

YAG:Ce crystals absorption in UV-visible spectral region are conditioned by the absorption of YAG
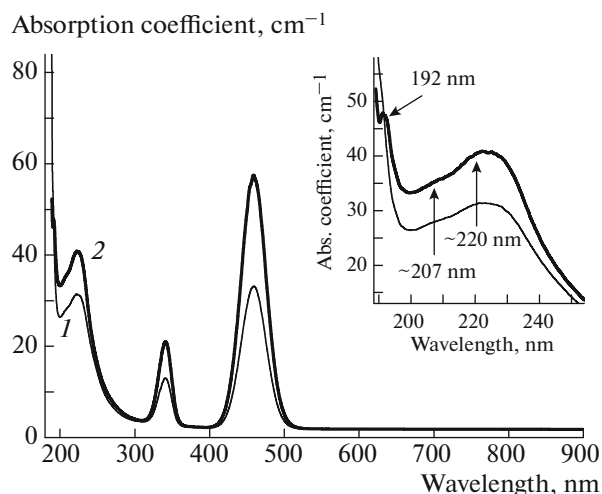

Fig. 1. (a) Absorption spectra of YAG before (*1*) and after (*2*) γ-irradiation, (b) γ-induced absorption spectra.

Fig. 2. Absorption spectra of YAG:Ce (0.12 (*1*) and 0.20 at % (*2*)) crystals. Inset: spectral position of the short-wave absorption bands of Ce^{3+}.
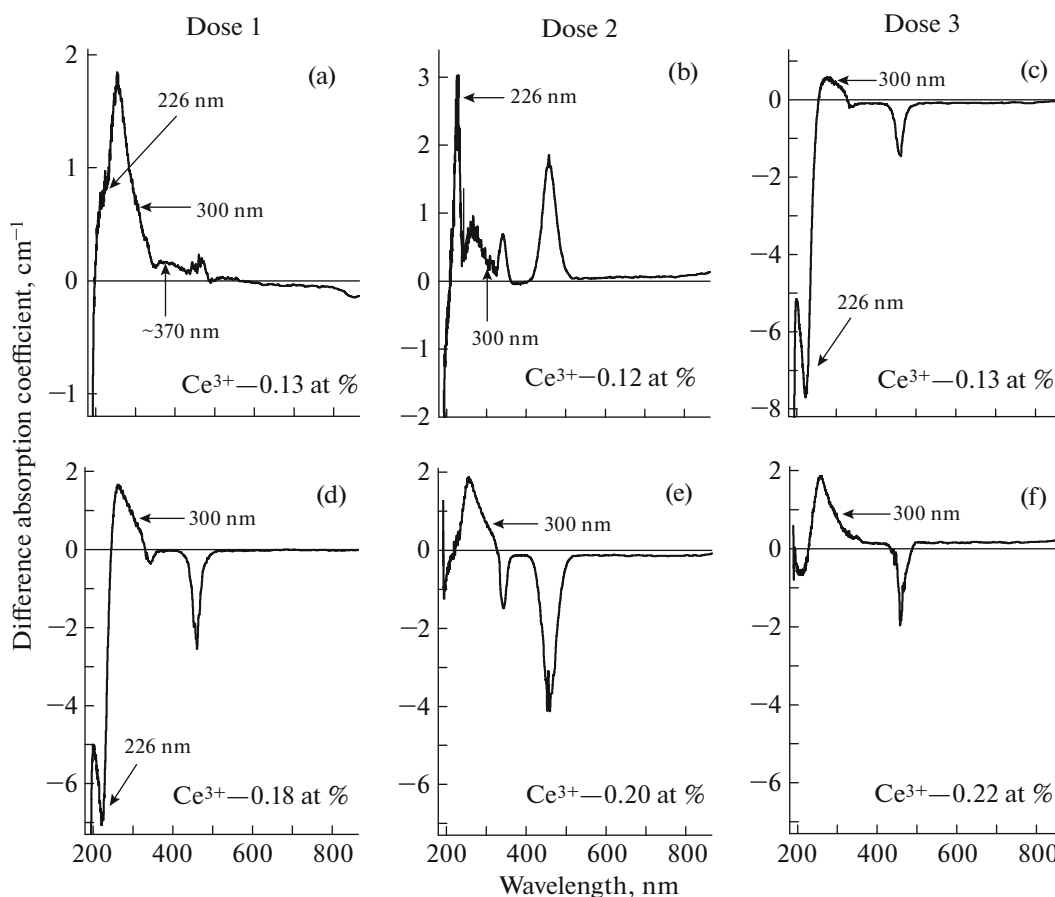
Fig. 3. γ-Induced absorption spectra of SC1 (a–c) and SC2 (d–f). Absorption changes of some color centers are indicated.

matrix, $4f^15d^0 \rightarrow 4f^05d^1$ transitions of Ce^{3+} and absorption of defects created by cerium ions. These crystals absorption spectra (Fig. 2) clearly exhibit only two bands of Ce^{3+} at 459 and 340 nm. Overlapping of Ce^{3+} absorption bands at ~220 nm [18, 22] and, probably, at ~207 nm [23] with the absorption of F^+ center (226 nm) is observed at attentive consideration of this range in inset on Fig. 2. The band at 192 nm which is enough discernible in the crystals with low absorption intensity at <190 nm and can be associated with Ce^{3+} transitions to the highest energy level located in the range of excitons creation [21, 23, 24].

The presence in YAG:Ce crystals of examined above color centers (or charge traps) which can be sources of electrons or holes for cerium ions were is not observed directly in the spectra on Fig. 2. But, such as in YAG crystal, the absorption of these centers arise in γ-induced spectra of YAG:Ce (SC1, SC2) which are presented in the next division.

Gamma-induced Absorption of YAG:Ce

Figure 3 depicts the spectra of γ-induced absorption of SC1 and SC2.

In comparison with YAG, about 10 times stronger absorption at 240–320 nm are seen in SC1 and, especially, in SC2 (Figs. 3a, 3d–3f). Besides the recharging band of Fe^{3+} at 240–260 nm [19], this range includes the absorption of T_{2g} triplet of Ce^{3+}_{Al} center at ~270–320 nm [11]. Increase of γ-induced absorption at 270–310 nm (Fig. 3a) can be interpreted by the formation of $(Ce^{4+}_{Al} + e)$ centers during the crystals irradiation, if to assume that Ce_{Al} defects in our crystals are forming in the crystallization process mainly as Ce^{4+}_{Al} adjacent to hole traps. The related absorption of $(Ce^{4+}_{Al} + e)$ center, hereinafter denoted as Ce^{3+}_{Al}, have been attributed to the band at ~300 nm located on the long-wave tail of the recharging band of Fe^{3+}. Increase of this band absorption in the crystals takes place under all applied doses (Fig. 3).

Intensity variation of γ-induced absorption of F^+ centers (~226 nm) accompanied by F centers (~196 nm) disintegration under certain doses (Figs. 3a, 3b) once more confirm theirs belonging to different kinds of the F type centers [25]. Besides the denoted defects, in γ-induced spectrum of SC1 is seen the absorption at
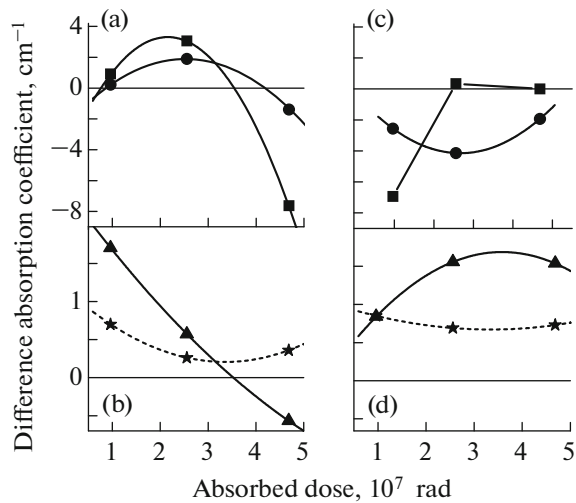
Fig. 4. Dependencies of γ–induced absorption changes of the bands at 459 (●), 226 (■), 250 (▲) and 300 nm (★) with the absorbed doses in SC1—(a, b) and SC2—(c, d).

~370 nm (Fig. 3a) which can be associated with O⁻ centers [19, 26].

Figure 4 shows the measured absorption changes of Ce^{3+} at 459 nm, F^+ centers at 226 nm, recharging band of Fe^{3+} at ~250 nm and of Ce^{3+}_{Al} at ~300 nm depending on the crystals absorbed doses. Radiation behavior of each of noted absorptions, with the exception of the band at 226 nm in SC2 (Fig. 4c), may be described by polynomial fittings and are satisfying by the same types of trinomial quadratic equations like (1) and (2) for Ce^{3+}:

$$\Delta k_1(Ce^{3+}) = -2.495 + 3.488x - 0.694x^2 \text{ (SC1), (1)}$$

$$\Delta k_2(Ce^{3+}) = -0.259 - 2.913x + 0.546x^2 \text{ (SC2), (2)}$$

where x is the absorbed dose of γ-rays, $\Delta k_{1,2}$ is the difference absorption coefficient, i.e. the γ-induced absorption coefficient. Although the dependences presented on Fig. 4 quite well describe qualitative changes of γ-induced absorption of the noted color centers, but are insufficient for their quantitative assessment. In really, it is possible to analyze only the equations (1) and (2) as we can calculate only the changes of Ce^{3+} content in the crystals. The concen-

tration changes ΔC of Ce^{3+} (positive Δk) and Ce^{4+} (negative Δk) in YAG:Ce crystals for each of used irradiation doses (Fig. 3) are presented in Table 2. At the same time, ΔC values characterize a quantity of the activator ions valence changes ($Ce^{3+} \leftrightarrow Ce^{4+}$) and allow to define the number (n) of those regular cerium ions which are susceptible to influence of the defects located near dodecahedral sites of cerium in unit volume of YAG:Ce.

As follows from Eq. (1), $Ce^{4+} \to Ce^{3+}$ transitions in SC1 (linear term $3.488x$) are simultaneously retarding by reverse transitions $Ce^{3+} \to Ce^{4+}$ (quadratic term $-0.694x^2$). And the constant term implies that not irradiated SC1 may contain about 9.7×10^{-3} at % of Ce^{4+} what is the reason of increase in intensity of Ce^{3+} absorption under doses 1 and 2 (Fig. 4a).

Radiation change of Ce^{3+} absorption in SC1 correlates with the behaviors of the bands at 226 nm (F^+ center) and at 250 nm (Figs. 4a, 4b) which characterize both formation and disintegration of F^+ centers and the transitions $Fe^{3+} \leftrightarrow Fe^{2+}$. On the other hand, radiation changes of the absorption of Fe^{3+} at ~250 nm correlates with the changes of Ce^{3+}_{Al} (300 nm) under doses 1 and 2 (Fig. 4b). Increase of the number of $Ce^{4+}_{Al} \to Ce^{3+}_{Al}$ and $Fe^{3+} \to Fe^{2+}$ processes under dose 3 is the result of electron loss by Ce^{3+} and disintegration of F^+ centers.

Radiation change of Ce^{3+} absorption in SC2 (Fig. 4c) shows a reduction of intensity of γ-induced absorption under all applied doses. From Eq. (2), on the contrary to Eq. (1), follow that transitions $Ce^{3+} \to Ce^{4+}$ in SC2 (linear term $-2.913x$) are simultaneously retarding by the reverse transitions $Ce^{4+} \to Ce^{3+}$ (quadratic term $0.546 x^2$). The constant term indicates that not irradiated SC2, practically, did not contain of Ce^{4+}. In addition, radiation behavior of the absorption change of Ce^{3+} ions in SC2 does not correlates with F^+ centers (226 nm) behavior, but close to the changes of Fe^{3+} and of Ce^{3+}_{Al} (Fig. 4d).

Table 2. Ce^{3+} and Ce^{4+} ions concentration changes in γ-irradiated YAG:Ce

Irradiation dose	SC1		SC2	
	$\Delta C(Ce^{3+})$, at %	$\Delta C(Ce^{4+})$, at %	$\Delta C(Ce^{3+})$, at %	$\Delta C(Ce^{4+})$, at %
1	0.85×10^{-3}	—	—	8.7×10^{-3}
2	7.3×10^{-3}	—	—	14×10^{-3}
3	—	5.4×10^{-3}	—	6.9×10^{-3}

Role of Cerium Content on the Radiation Behavior of Ce^{3+} in YAG:Ce

Relatively large ionic radius of Ce^{3+} (r^{VIII}–1.14 Å), as compared to Y^{3+} (r^{VIII}–1.02 Å), induces a local distortion of a part of dodecahedral sites of Ce^{3+} in YAG:Ce. It leads to the stabilization of some crystal defects nearby the activator ions in a process of the crystals growing. As follows from Fig. 4, almost twice as much of Ce^{3+} ions content in as-grown crystals produce the different changes of γ-induced absorption not only of Ce^{3+} but also of examined color centers. The raised content of Ce^{4+} (r^{VIII}–0.97 Å) in as-grown SC1 indicates a presence of about the same number of hole traps close to the dodecahedral site of these ions. And opposite, almost complete absence of Ce^{4+} in as-grown SC2 means that an increasing of Ce^{3+} concentration leads to suppressing of hole traps formation around the activator sites, since Ce^{3+} by themselves also represents the hole trap.

Equations (1) and (2) which describe the changes of γ-induced absorption of Ce^{3+} in SC1 and SC2 may be represented as the sum of negative and positive changes of Ce^{3+} absorption as:

$$\Delta k_1(Ce^{3+}) = \Delta k_1^1 + \Delta k_1^2 \quad (SC1),$$

$$\Delta k_2(Ce^{3+}) = \Delta k_2^1 + \Delta k_2^2 \quad (SC2),$$

where $\Delta k_1^1 = 3.49x$; $\Delta k_1^2 = -(2.49 + 0.69x^2)$; $\Delta k_2^1 = -(0.26 + 2.91x)$; $\Delta k_2^2 = 0.54x^2$. The positive values Δk_1^1 and Δk_2^2 define the absorption of that number $\Delta n_1^1(Ce^{3+})$ and $\Delta n_2^2(Ce^{3+})$ of Ce^{3+} which have been created by irradiation. The negative values Δk_1^2

and Δk_2^1 define the negative absorption of that number $\Delta n_1^2(Ce^{4+})$ and $\Delta n_2^1(Ce^{4+})$ of Ce^{3+}, which have been recharged to Ce^{4+}. After a recalculation of these additional absorption coefficients to the number of Ce^{3+} and Ce^{4+} ions in unit volumes of the crystals, the common quantity Δn_1 and Δn_2 of these ions or the number of $Ce^{4+} \rightarrow Ce^{3+}$ and $Ce^{3+} \rightarrow Ce^{4+}$ transitions in 1 cm^3 in SC1 and SC2 can be written as

$$\Delta n_1 = \Delta n_1^1(Ce^{3+}) + \Delta n_1^2(Ce^{4+}) \quad (SC1), \qquad (3)$$

$$\Delta n_2 = \Delta n_2^1(Ce^{4+}) + \Delta n_2^2(Ce^{3+}) \quad (SC2), \qquad (4)$$

where $\Delta n_1^1 = 0.94 \times 10^{11}x$; $\Delta n_1^2 = 0.67 \times 10^{18} + 1.86 \times 10^3 x^2$; $\Delta n_2^1 = 0.77 \times 10^{11}x$; $\Delta n_2^2 = 1.40 \times 10^3 x^2$.

As shown on Fig. 5, the equations (3) and (4) describe mechanisms of radiative creation of Ce^{3+} and Ce^{4+} in SC1 (curves 1 and 2) and in SC2 (curves 4 and 3). The difference between quantity of Ce^{3+} and Ce^{4+} ions, created under the crystals irradiation by doses 1, 2 and 3, is equivalent to resultant changes of Ce^{3+} concentration (Table 2) and absorption intensity at 459 nm (the positive or negative Δk) (Figs. 3 and 4) in SC1 and SC2. So, the obtained dependencies (curves 1–4) give an opportunity to predict the changes of γ-induced absorption of Ce^{3+} for each of absorbed doses in the range $(0.5–5) \times 10^7$ rad.

For determination of the concentration of electron–hole traps participating in a recharge of the activator, let's consider the derivatives of the equations (3) and (4), where x is replaced by γ-photons number absorbed by cerium ions (Table 1). The components of these $(\Delta n_1)'$ and $(\Delta n_2)'$ derivatives, plotted as separable dependences 1–4 on Figs. 6a, 6b, describe evolution
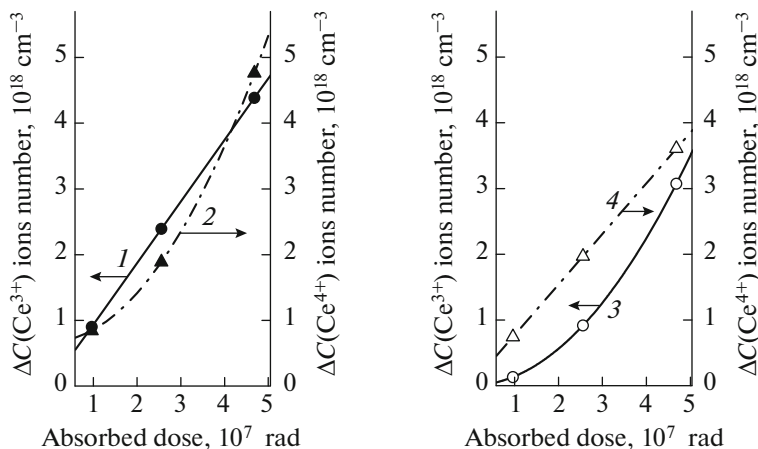

Fig. 5. Radiative change of Ce^{3+} (●, ○) and Ce^{4+} (▲, △) number in SC1 and SC2 with the crystals absorbed dose. Curves 1, 2 for SC1 and 3, 4 for SC2 are described by the equations (3) and (4). ● (1)—$\Delta n_1^1(Ce^{3+})$, ▲ (2)—$\Delta n_1^2(Ce^{4+})$, ○ (3)—$\Delta n_2^2(Ce^{3+})$, △ (4)—$\Delta n_2^1(Ce^{4+})$.
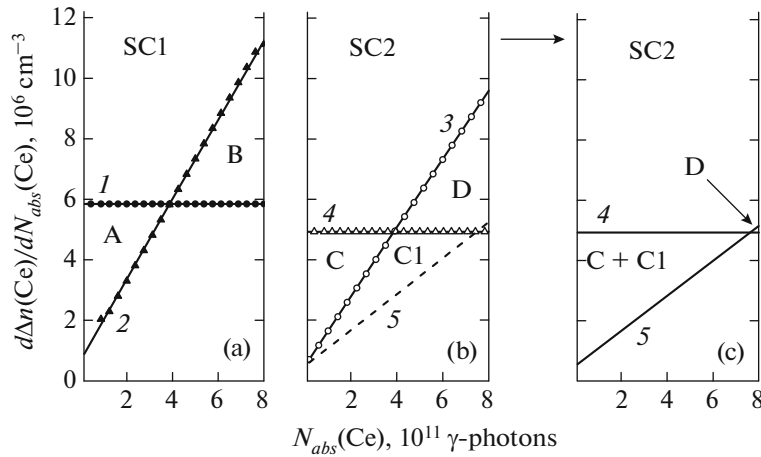
Fig. 6. Derivatives of the quantity of Ce^{3+} (*1, 3, 5*) and Ce^{4+} (*2, 4*) changes with respect of absorbed γ-photons by cerium ions in SC1 (a) and SC2 (b, c). (A, D) Ranges of e-centers participation; (B, C, C1) ranges of h-centers participation.

dynamics of the recharging processes $Ce^{3+} \leftrightarrow Ce^{4+}$ in SC1 and SC2 within the limit of irradiation range $(0.6{-}8) \times 10^{11}$ γ-photons.

The processes of an electron capturing by Ce^{4+} ($Ce^{4+} \rightarrow Ce^{3+}$) in SC1 and of a hole capturing by Ce^{3+} ($Ce^{3+} \rightarrow Ce^{4+}$) in SC2 (curves *1* and *4* on Fig. 5) defined by the linear terms $\Delta n_1^1(Ce^{3+})$ and $\Delta n_2^1(Ce^{4+})$ in equations (3) and (4), take place with constant increments $(\Delta n_1^1(Ce^{3+}))'$ and $(\Delta n_2^1(Ce^{4+}))'$ (horizontal curves *1* and *4* on Fig. 6). These increments are 5.8×10^6 cm^{-3} per γ-photons in SC1 and 4.9×10^6 cm^{-3} per γ-photons in SC2. Integral number of the radiation created Ce^{3+} in SC1 and Ce^{4+} in SC2 are equal to the areas under horizontal curves *1* and *4* on Figs. 6a, 6b. The competing reverse processes of a hole capturing by Ce^{3+} ($Ce^{3+} \rightarrow Ce^{4+}$) in SC1 and an electron capturing by Ce^{4+} ($Ce^{4+} \rightarrow Ce^{3+}$) in SC2 (curves *2* and *3* in Fig. 5) defined by the square terms $\Delta n_1^2(Ce^{4+})$ and $\Delta n_2^2(Ce^{3+})$ in equations (3) and (4), evolve with accelerations (not horizontal curves *2* and *3* in Figs. 6a, 6b) and are described as

$$\left(\Delta n_1^2(Ce^{4+})\right)' = 0.71 \times 10^6 \\ + 1.32 \times 10^{-5} N_{abs}(Ce) \quad (SC1), \tag{5}$$

$$\left(\Delta n_2^2(Ce^{3+})\right)' = 0.47 \times 10^6 \\ + 1.14 \times 10^{-5} N_{abs}(Ce) \quad (SC2). \tag{6}$$

Integral numbers of the radiation created Ce^{4+} in SC1 and Ce^{3+} in SC2 are equal to the areas under not horizontal dependences *2* and *3* on Figs. 6a, 6b.

Radiation processes $Ce^{3+} \leftrightarrow Ce^{4+}$ in the crystals reach equilibrium at a cross point at the doses 3.89×10^{11} γ-photons for SC1 (Fig. 6a) and at 3.91×10^{11} γ-photons for SC2 (Fig. 6b). At these doses take place

the quantity equivalence of the changeable Ce^{3+} and Ce^{4+} as well as of the concentrations of electron and hole traps. The difference between the areas under curves *1* and *2* (triangles A and B on Fig. 6a) as well as between the areas under curves *3* and *4* (triangles C and D on Fig. 6b) define the quantity of defects closely spaced to the activator ions in as grown crystals and influencing a valence state of cerium ions during the crystals irradiation. Magnitudes of the areas of noted triangles S_A and S_B in SC1 and S_C and S_D in SC2, the initial content of electron-hole traps and Ce_{Al} content in the crystals are presented in Table 3. The numbers of Ce^{3+} disposed near hole centers in as-grown SC1 and of Ce^{4+} disposed near electron centers in as-grown SC2 are equal to the constant components of $(\Delta n_2^2(Ce^{3+}))'$ and $(\Delta n_1^2(Ce^{4+}))'$ in Eqs. (5) and (6).

The area of S_A, where the number of ($Ce^{4+} + e$) > ($Ce^{3+} + h$), determines the quantity of electron centers disposed near Ce^{4+} in SC1 which are turning into hole centers in the result of electron capture by Ce^{4+}. The area of S_B, where the number of ($Ce^{3+} + h$) > ($Ce^{4+} + e$), determines the quantity of hole centers created by radiation in SC1. The difference between quantities of electron and hole centers ($S_B - S_A$) testifies about an occurrence of additional hole centers, number of which corresponds to the content of Ce_{Al} (3–6% of the regular cerium ions concentration [10]) in these crystals (Table 3). As shown on Fig. 4b, in SC1 are observed only $Ce_{Al}^{4+} \rightarrow Ce_{Al}^{3+}$ processes under the crystals irradiation. The holes, ejected by Ce_{Al}^{4+} and captured by nearest electron centers, convert them to hole centers. Formation of such additional radiation centers is resulting in the acceleration of the processes of hole transfer to Ce^{3+} in SC1 (curve *2* on Fig. 6a).

Table 3. Quantity[1−3] of charge traps interacting with Ce^{3+}, Ce^{4+} and Ce_{Al} in YAG:Ce

Crystals	C_{Ce}	Centers in as-grown crystals			Radiation changed centers		
		e-center near Ce^{4+}	h-center near Ce^{3+}	Ce_{Al} [10]	e-center near Ce^{4+}	h-center near Ce^{3+}	e-center near Ce_{Al}^{4+}
SC1	~86.5 (~125)	6.7 (9.7)	0.7 (1)	~3.4 (4.9)	S_A 7.6 (11)	S_B 11.2 (16)	S_B-S_A 3.6 (5.0)
SC2	~138.7 (~200)	0.5 (0.72)	5.4 (7.8)	~6.9 (9.9)	S_D − (−)	S_C 6.6 (9.1)	S_{C1} ~6.9 (9.9)

[1] Quantity of charge traps are given in units 10^{17} cm^{-3} and 10^{-3} at % (in brackets).
[2] Concentration of Ce_{Al} centers has been calculated as a part [10] of Ce^{3+} in crystals.
[3] Values of $S_{A,B,C,C1}$ have been calculated for the irradiation range $(0.6-8) \times 10^{11}$ γ-photons.

In comparison with SC1, antithetic radiation behavior of the activator ions and decreased number of all recharging processes are observed in SC2 (Fig. 6b). The area of S_C, where the number of $(Ce^{3+} + h) > (Ce^{4+} + e)$, defines the number of hole centers disposed near Ce^{3+} in SC2. The area of S_D defines the number of electron centers which would be formed in SC2 under dose 3. But we did not observe any additional increasing of absorption bands intensity of Ce^{3+} ions in SC2 under used irradiation doses (Figs. 3d–3f) what indicate the appearance of additional hole centers (electron traps) around Ce^{3+} under the crystals irradiation.

It should be noted that investigated YAG and YAG:Ce crystals had been grown by the same method and by using of the same row materials. The principal distinction between SC1 and SC2 include the intense absorption at 230−320 nm which is repeating in γ-induced absorption spectra and the increased number of Ce^{4+} in SC2 under all irradiation doses. The reason of this effect can be, most of all, explained by twice increased content of Ce_{Al}^{4+} centers (Table 3). In this case, like in SC1, the recharging $Ce_{Al}^{4+} \rightarrow Ce_{Al}^{3+}$ processes promote formation of additional hole centers (triangle C1 on Fig. 6b), quantity of which is defined by the area S_{C1} (Table 3). Thus, the increase of hole centers number $(S_C + S_{C1})$ suppress a formation of new electron centers near dodecahedral sites of cerium, transform the dependence *3* to the dependence *5* and the recharging $Ce^{3+} \leftrightarrow Ce^{4+}$ processes in SC2 will reach equilibrium at a cross point under higher dose (Fig. 6c).

As shown on Figs. 3e, 3f and 4c, 4d, γ-induced absorption observed in SC2 under doses 2 and 3 is the absorption result only of one electron center (Ce_{Al}^{3+}) and of one hole center (Fe^{3+}). Therefore, only the radiative recharging processes $Ce_{Al}^{4+} \rightarrow Ce_{Al}^{3+}$ can be the source of appearance of additional hole centers in SC2. These data suggest that rise of the dopant content (0.18−0.23 at %) in as-grown crystals leads to the absence of Ce^{4+} and to the presence of only electron traps in surrounding of ~4% of Ce^{3+}, which are equilibrate the hole traps around of Ce_{Al}^{4+}. The total number of $Ce^{3+} \leftrightarrow Ce^{4+}$ recharging processes, conditioned by the existence of these defects, is equal to ~13.5 × 10^{17} cm^{-3}.

Completely another distribution and quantity of defects are observed in SC1 (Table 3) with comparatively low concentration of Ce^{3+} (0.12−0.13 at %). These crystals contain excess number of hole traps (~10 times more than electron traps) around of the activator site and ~3.6 × 10^{17} cm^{-3} nearby Ce_{Al}^{4+}. About 8% from the total concentration of cerium can exist in these crystals as Ce^{4+}. The number of all recharging processes $Ce^{3+} \leftrightarrow Ce^{4+}$, conditioned by the existence of these defects, is equal to ~18.8 × 10^{17} cm^{-3} what is ~30% more than in SC2.

CONCLUSIONS

Impact of γ-rays $((1.13-5.5) \times 10^7$ rad) on YAG:Ce (0.12−0.22 at %) single crystals leads to an occurrence of the competing reverse $Ce^{3+} \leftrightarrow Ce^{4+}$ recharging processes by reason of actively interaction of a part of Ce^{3+} with the intrinsic defects localized near dodecahedral site of the activator in as-grown crystals. Presented in this work the methodology of a quantity estimation of the noted recharging processes and mechanisms consideration of their evolution give information on quantity of the charge traps formed in as-grown crystals and then involved in radiative processes of the activator recharging. This data allow forecasting changes of the activator ions absorption for each of doses in noted range of γ-irradiation. Decisive role in a formation of color centers in as-grown YAG:Ce plays the concentration of cerium ions which "manage" the crystals

defects distribution and a ratio of electron and hole traps around themselves. Introduction of Ce^{3+} (up to ~0.15 at %) in these crystals stimulates the formation of excessive number of cation vacancies due to large ionic radius of Ce^{3+}. And on the contrary, the increasing of dopant concentration suppresses the formation of the crystals cation vacancies in the result of corresponding increase of Ce^{4+}_{Al} number which promote a reduction of color centers content, improve the nearest environment of the dodecahedral site of Ce^{3+} ions and heighten radiation stability of these crystals.

ACKNOWLEDGMENTS

REFERENCES

1. M. Moszynski, M. Kapusta, M. Mayhugh, D. Wolski, and S. O. Flyckt, IEEE Trans. Nucl. Sci. NS-44, 1052 (1997).
2. J. A. Mares, M. Nikl, A. Beitlerova, C. D'Ambrosio, F. de Notaristefani, K. Blazek, P. Maly, and K. Nejezchleb, Optical Materials 24, 281 (2003).
3. W. Chewpraditkul, L. Swiderski, M. Moszynski, T. Szczesniak, A. Syntfeld-Kazuch, C. Wanarak, and P. Limsuwan, Phys. Stat. Sol. A 206 (11), 2599 (2009).
4. M. Globus, B. Grinyov, V. Lyubynskiy, and T. Hrynova, in Problems of Atomic Science and Technology. Series: Physics of Radiation Damage, Radiative Study of Materials (2003), No. 6 (84), pp. 89–97 [in Russian].
5. J. S. Stroud, J. Chem. Phys. 35 (3), 844 (1961).
6. J. S. Stroud, J. Chem. Phys. 37 (4), 836 (1962).
7. T. Butaeva, A. Petrosyan, I. Gambaryan, A. Vardanyan, M. Mkrtchyan, C. Pedrini, and C. Dujardin, in Frontiers in Optics (FiO)/Laser Science (LS) (Optical Society of America, Washington, 2011), JWA14.
8. S. M. Kaczmarek, G. Domianiak-Dzik, W. Ryba-Romanowski, J. Kisielewski, and J. Wojtkowska, J. Cryst. Res. Technol. 34 (8), 1031 (1999).
9. S. M. Kaczmarek, M. Berkowski, Z. Moroz, and S. Warchol, Acta Physica Polonica 96 (3–4), 417 (1999).
10. V. V. Laguta, A. M. Slipenyuk, M. D. Glinchuk, I. P. Bykov, Y. Zorenko, M. Nikl, J. Rose, and K. Nejezchleb, Radiat. Meas. 42, 835 (2007).
11. V. Babin, V. V. Laguta, A. Makhov, K. Nejezchleb, M. Nikl, and S. Zazubobovich, Nuclear Science, IEEE 55 (3), 1156 (2008).
12. V. Babin, P. Fabeni, A. Krasnikov, K. Nejezchleb, M. Nikl, G. P. Pazzi, T. Savikhina, and S. Zazubovich, J. of Lumin. 124 (2), 273 (2007).
13. K. L. Ovanesyan, G. O. Shirinyan, A. G. Petrosyan, C. Dujardin, C. Pedrini, M. Mkrtchyan, and A. Grigoryan, in Proceedings of the Conference "Laser Physics—2007" (Armenia, Institute for Physical Research NAS of RA, 2007), pp. 20–23.
14. I. V. Vereshchinsky and A. K. Pikaev, Introduction in Radiation Chemistry (Akad. Nauk SSSR, Moscow, 1963) [in Russian].
15. J. H. Hubbell and S. Seltzer, Intern. J. Appl. Radiation and Isotopes 33, 1269 (1982).
16. S. R. Rotman, C. Warde, H. L. Tuller, and J. Haggerty, J. Appl. Phys. 66 (1), 3207 (1989).
17. W. F. Krupke, IEEE J. Qunt. Elect. QE-7 (4), 153 (1971).
18. C. M. Wong, S. R. Rotman, and C. Warde, J. Appl. Phys. Lett. 44 (11), 1038 (1984).
19. I. Sh. Akhmadullin, S. A. Migachev, and S. P. Mironov, Nucl. Inst. Meth. Phys. Res. B65, 270 (1992).
20. A. Pujats and M. Springis, Rad. Eff. Def. Sol. 155 (1–4), 65 (2001).
21. M. Kirm, A. Lushchik, Ch. Lushchik, and G. Zimmerer, ECS Proceedings 99–40, 113 (2000).
22. W. J. Miniscalco, J. M. Pellegrino, and W. M. Yen, J. Appl. Phys. 49 (12), 6109 (1978).
23. P. A. Tanner, L. Fu, L. Ning, B.-M. Cheng, and M. G. Brik, J. Phys.: Condens. Matter 19, 216213 (2007); http://dx.doi.org/. doi 10.1088/0953-8984/19/21/216213
24. V. Mark and N. Yaroshevich, in Proceedings of the International Conference on Inorganic Scintillators and Their Applications (SCINT—95) (Delft Univ. Press, 1996), pp. 359–361.
25. K. H. Lee and J. H. Crawford, Phys. Rev. B15 (8), 4065 (1977).
26. J. Kvapill, J. Kvapill, and B. Perner, Kristall Technik 10 (2), 161 (1975).